Wen, Y., Liu, Z., Lin, S., Chen, Y., Zhang, Y., & Yu, S. (2018). Construction, characteristics, and constraints of accelerating beams based on caustic design. *Optics Express*, *26*(25), 32728-32738. https://doi.org/10.1364/OE.26.032728

Research Article | Vol. 26, No. 25 | 10 Dec 2018 | OPTICS EXPRESS 32728
Optics EXPRESS

Construction, characteristics, and constraints of accelerating beams based on caustic design

YUANHUI WEN,[1,3] ZHIBIN LIU,[1,3] SHUQING LIN,[1,3] YUJIE CHEN,[1,*] YANFENG ZHANG,[1] AND SIYUAN YU[1,2]

[1]*State Key Laboratory of Optoelectronic Materials and Technologies, School of Electronics and Information Technology, Sun Yat-sen University, Guangzhou 510275, China*
[2]*Photonics Group, Merchant Venturers School of Engineering, University of Bristol, Bristol BS8 1UB, UK*
[3]*These authors contributed equally*
[*]*chenyj69@mail.sysu.edu.cn*

Abstract: Caustic methods have been proposed for wavefront design to enable light beams propagating along curved trajectories, namely accelerating beams. Here we elaborate the complete construction, remarkable characteristics, and hidden constraints of these methods. It is found that accelerating beams based on the caustic design have not only a well-known curved intensity distribution but also a linear phase distribution along the caustic proportional to the curved length, as if light field indeed moved along the caustic. Moreover, with this characteristic, further light-ray analyses are implemented to illustrate the constraints of caustic design in different cases. We expect our work will clarify some confusion on the effectiveness and applicability of caustic methods, and thus facilitate the design of accelerating beams for various applications.

1. Introduction

Structured light [1] with elaborate design of initial field distribution may possess some extraordinary properties, such as self-accelerating [2,3], nondiffracting [4], and even carrying orbital angular momentum [5], which reveals the abundance of a light beam in the space or space-time [6] domain. In particular, self-accelerating beams are a kind of light beams propagating along curved trajectories in free space [2,3,7–10], which have been studied intensively in recent years. This is not only because such beams are fascinating as they seemingly violate the axiom of light propagation along straight lines, but also they can be useful in a variety of applications using light beams for energy, substance or information delivery along arbitrary trajectories, including micro-machining [11], particle-manipulation [12,13], optical communications [14,15], imaging [16,17], and laser assisted guiding of some processes such as filamentation [18] and electric discharges [19].

Since the above-mentioned applications take advantage of light beams propagating along curved trajectories, it is critical to enable the possibility of tailoring accelerating beams with various propagating trajectories, beyond the parabolic type of the first discovered accelerating Airy beam in the paraxial regime [2,3]. To this end, caustic methods [20] that associate the desired propagating trajectory with a caustic, namely the envelope of a family of light rays [21], have been proposed. This method was first demonstrated with real-space design in the paraxial regime and achieved on-demand convex propagating trajectories for two-dimensional (2D) light fields [22]. Later it has been widely extended, from real-space design to Fourier-space design [23] and even phase-space design [24], from paraxial regime to nonparaxial regime [25], from convex trajectories to nonconvex trajectories [26,27], from 2D light fields to 3D light fields [28,29], and from the phase-only modulation to the combined phase and amplitude modulation [30,31]. Such scheme does greatly extend the available

#345213 https://doi.org/10.1364/OE.26.032728
Journal © 2018 Received 6 Sep 2018; revised 6 Nov 2018; accepted 7 Nov 2018; published 28 Nov 2018

Optics EXPRESS

propagating trajectories, and therefore there is often a claim in some papers that arbitrary propagating trajectories are obtainable, which is actually not the case. In this work, we elaborate the complete construction, remarkable characteristics, and hidden constraints of accelerating beams that are designed based on caustic methods, which may clarify some confusion about the applicability of these methods in the design of accelerating beams.

2. Construction and characteristics of accelerating beams from light-ray perspective

2.1 Light-ray model based on stationary phase approximation

In general, the propagation of a light beam in free space can be characterized based on the plane-wave (angular spectrum) decomposition. In the case of 2D light field $E(x,z)$ discussed in this work, (i.e. light field distribution independent of y direction), the angular spectral integral can be expressed as

$$E(x,z)=\int A(k_x)\exp\{i[k_x x+(k^2-k_x^2)^{1/2}z]\}dk_x=\int r(k_x)\exp[i\Psi(k_x)]dk_x, \quad (1)$$

where $k=2\pi/\lambda$ is the vacuum wave number with $\lambda=632.8$ nm in this paper, k_x is spatial angular frequency with $k_x<k$ corresponding to propagating plane wave; $A(k_x)=r(k_x)\exp[i\Phi(k_x)]$ is the angular spectrum in the initial plane $z=0$, with $r(k_x)$ and $\Phi(k_x)$ representing its amplitude and phase distribution, respectively, and $\Psi(k_x)=k_x x+(k^2-k_x^2)^{1/2}z+\Phi(k_x)$. According to the principle of stationary phase approximation [32], suppose the phase distribution $\Psi(k_x)$ varies much faster than the amplitude distribution $r(k_x)$, the contribution to the above integral mainly comes from the stationary point of $\Psi(k_x)$, namely the point k_{x1} satisfying

$$\Psi'(k_{x1})=x-\frac{k_{x1}}{(k^2-k_{x1}^2)^{1/2}}z+\Phi'(k_{x1})=0. \quad (2)$$

Note that the light field at different position (x,z) with the same k_{x1} value falls into a straight line. Furthermore, if we take the second-order Taylor expansion of the phase function $\Psi(k_x)$ in Eq. (1) at the stationary point k_{xm}, the field distribution can be simplified as

$$E(x,z)=\sum_m r(k_{xm})\cdot\left(\frac{2\pi}{|\Psi''(k_{xm})|}\right)^{1/2}\cdot\exp\left\{i\Psi(k_{xm})+i\cdot sign[\Psi''(k_{xm})]\cdot\frac{\pi}{4}\right\}, \quad (3)$$

where m is the mth stationary point if more than one stationary point exist, and $sign[x]$ = 1 (if x is positive) or −1 (if x is negative). The field distribution in Eq. (3) can be intuitively interpreted as the superposition of the light rays described by Eq. (2) as shown in Fig. 1(a), with a normal phase evolution $\Psi(k_{xm})=k_{xm}x+(k^2-k_{xm}^2)^{1/2}z+\Phi(k_{xm})$ due to the propagation of the light ray. However, it is noted that there is an additional phase shift in Eq. (3), with a value of $\pi/4$ or $-\pi/4$ depending on the sign of $\Psi''(k_{xm})$ [33], which would have some significant effects as discussed in the following.

Optics EXPRESS

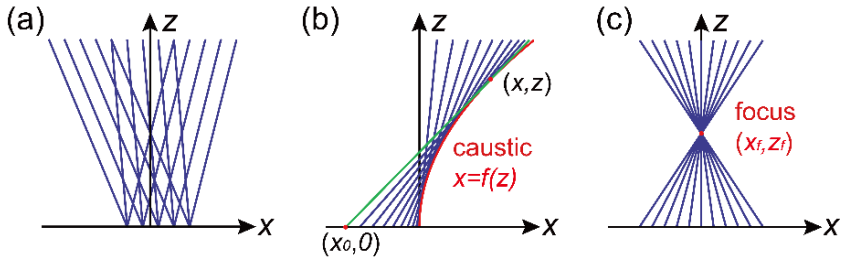

Fig. 1. Schematic showing the light-ray picture if (a) $\Psi'(k_x)=0$, (b) $\Psi'(k_x)=0$ and $\Psi''(k_x)=0$, (c) $\Psi'(k_x)=0$, $\Psi''(k_x)=0$, and $\Psi'''(k_x)=0$, which correspond to the light rays emanating randomly, forming a caustic, and focusing, respectively.

2.2 Convex type of caustic beams

Based on the above light-ray analysis, a caustic as shown in Fig. 1(b), can be obtained by setting the second derivative of $\Psi(k_x)$ to be zero:

$$\Psi''(k_{x1})=-\frac{k^2}{(k^2-k_{x1}^2)^{3/2}}z+\Phi''(k_{x1})=0. \tag{4}$$

This is attributed to the fact that Eqs. (2) and (4) can jointly result in a relation $x=f(z)$ after eliminating the variable k_{x1}, and this curve $x=f(z)$ satisfies:

$$f'(z)=\frac{dx}{dz}=\frac{k_{x1}}{(k^2-k_{x1}^2)^{1/2}}+\frac{k^2}{(k^2-k_{x1}^2)^{3/2}}z\cdot\frac{dk_{x1}}{dz}-\Phi''(k_{x1})\cdot\frac{dk_{x1}}{dz}=\frac{k_{x1}}{(k^2-k_{x1}^2)^{1/2}}, \tag{5}$$

indicating that each light ray is tangential to this curve and thus forms a caustic $x=f(z)$ as shown in Fig. 1(b). Since the light field near the caustic is intensive, accelerating beams can be designed by associating the desired propagating trajectory with a caustic. Once the caustic $x=f(z)$ is determined, the initial phase distribution $\Phi(k_x)$ can be obtained by solving Eqs. (2) and (5), a caustic method that has been widely used for the design of accelerating beams propagating along various trajectories [23]. However, the above method requires a one-to-one correspondence between k_{x1} and z in order to be solvable, which limits the available caustics to the convex type (including the concave one), namely light beams bending toward only one direction without bending back as shown in Fig. 1(b).

It is also interesting to find that if we further require the third derivative of $\Psi(k_x)$ to be zero:

$$\Psi'''(k_{x1})=-\frac{3k^2k_x}{(k^2-k_{x1}^2)^{5/2}}z+\Phi'''(k_{x1})=0. \tag{6}$$

It corresponds to the case of focusing, with a focal point $(x,z)=(x_f,z_f)$ under the phase distribution $\Phi(k_{x1})=-k_{x1}x_f-(k^2-k_{x1}^2)^{1/2}z_f$, as shown in Fig. 1(c).

2.3 Phase distribution along caustic

Although enhanced intensity around a caustic has been recognized for some time [34] and recently employed for the construction of accelerating beams [20–31], to the best of our knowledge, the discussion on the phase distribution along the caustic is missing in the literature, which is actually an important and elegant characteristic as pointed out in this

work. The phase of the light field on the caustic can be calculated based on the aforementioned analysis (Appendix A), which is found to be

$$\Psi(k_{x1}) = k_{x1}x + (k^2 - k_{x1}^2)^{1/2} z + \Phi(k_{x1}) = k \cdot \int \sqrt{1 + [f'(z)]^2}\, dz. \tag{7}$$

It is interesting that the phase on the caustic is proportional to the length of the curve, namely increases linearly along the curve, as if light just propagated exactly along the caustic. Therefore, design of accelerating beams based on this caustic method will not only enable an intensive curved main lobe, but also a linear phase distribution along it, an elegant characteristic that has been neglected before.

To confirm such theoretical analysis, two kinds of common accelerating beams propagating along a parabola $x = f(z) = a \cdot z^2$ (a is a parameter) and a circle $x = f(z) = \pm\sqrt{r^2 - (z - z_0)^2} + x_0$ (r, x_0, z_0 are parameters) are constructed based on the above caustic method, with the following designed angular spectra in the initial plane

$$\begin{aligned} &\text{parabola}: \ A(k_x) = \frac{1}{1-(k_x/k)^2} \exp\left\{ i\left[k \cdot \operatorname{artanh}(k_x/k) - k_x \right] / 4a \right\}, \\ &\text{circle}: \quad A(k_x) = \frac{1}{\sqrt{1-(k_x/k)^2}} \exp\left\{ i\left[\mp k \cdot r \cdot \arcsin(k_x/k) - k_x x_0 - \sqrt{k^2 - k_x^2}\, z_0 \right] \right\}. \end{aligned} \tag{8}$$

Their propagation dynamics is shown in Fig. 2. As expected, the main lobes of these beams propagate along the designed trajectories with linearly increased phase accumulation, as if simple phase accumulation due to curved propagation.

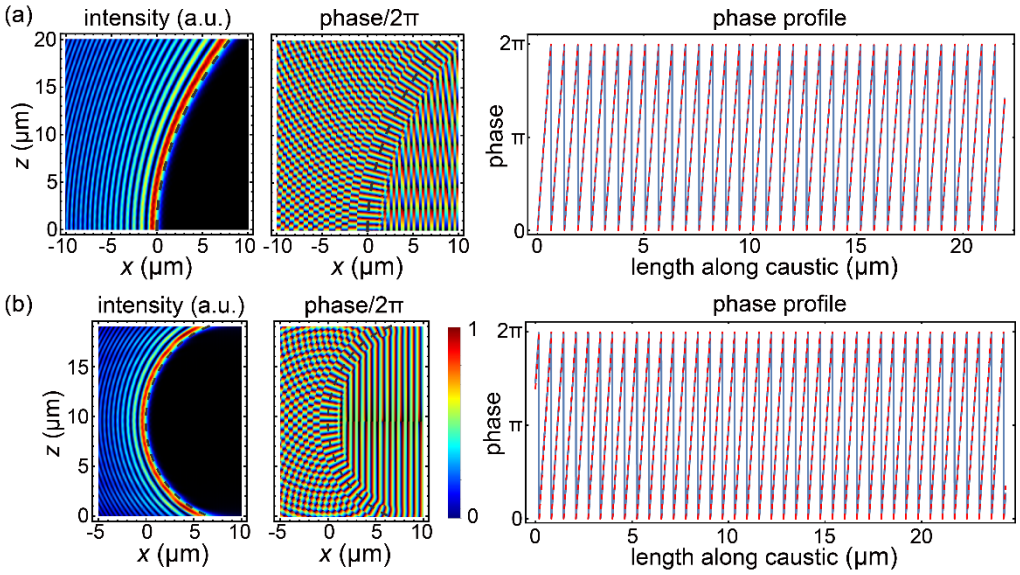

Fig. 2. Intensity and phase distributions as well as phase profiles of the constructed accelerating beams propagating along (a) a parabola (parameters: $x = 0.02z^2, |k_x| < 0.98k$, here x and z in unit of μm) and (b) a circle (parameters: $r = x_0 = 10\mu m, z_0 = 9.4\mu m, |k_x| < 0.98k$), based on the caustic method. The caustics are represented by dashed curves. The phase profiles along these caustics are depicted on the right in blue lines, matching well with red dashed lines indicating the phase accumulation of an imaginary light ray propagating along the caustics.

Optics EXPRESS

The above result will facilitate our understanding of the characteristics of accelerating beams in the perspective of two-ray interference, as illustrated in Fig. 3(a). On the right side of the caustic, there is no light ray passing by, which corresponds to an area with negligible intensity, while on the left side of the caustic, the light field at each point can be regarded as the interference of the two rays passing through this point and tangential to the caustic. The phase difference $\varphi_{12} = \varphi_1 - \varphi_2$ of these two rays at this point, e.g. point C in Fig. 3(a) will determine whether they interfere constructively or destructively, which can be directly expressed as

$$\varphi_{12} = k \cdot (l_{\overline{AC}} + l_{\overline{BC}} - l_{\overset{\frown}{AB}}) - \pi / 2. \tag{9}$$

The additional phase difference $-\pi/2$ is attributed to the additional phase shift $sign[\Psi''(k_{xm})] \cdot \pi/4$ as indicated in Eq. (3). For a light ray before touching the caustic, $\Psi''(k_{xm}) > 0$ so it has a $\pi/4$ phase, while after it touches the caustic, $\Psi''(k_{xm}) < 0$ so it has a $-\pi/4$ phase, namely resulting in a $-\pi/2$ phase difference. To justify the above formula, we have simulated the propagation of a circular beam as shown in Fig. 3(b). By adjusting the point C for $\varphi_{12} = 0, 2\pi, 7\pi, 20\pi$ corresponding to the white label 1, 2, 3, 4 in Fig. 3(b), respectively, one can see that the point locates exactly at the main lobe, the first side lobe, the fourth dark lobe, and the tenth side lobe as expected, which confirms the validity of treating accelerating beams as a two-ray interference based on Eq. (9). Moreover, it is noted that the main lobe corresponding to $\varphi_{12} = 0$ is not exactly on the caustic but having a small distance to it. As the point C approaches to point D on the caustic, the two rays no longer interfere completely constructively because of the $-\pi/2$ phase difference.

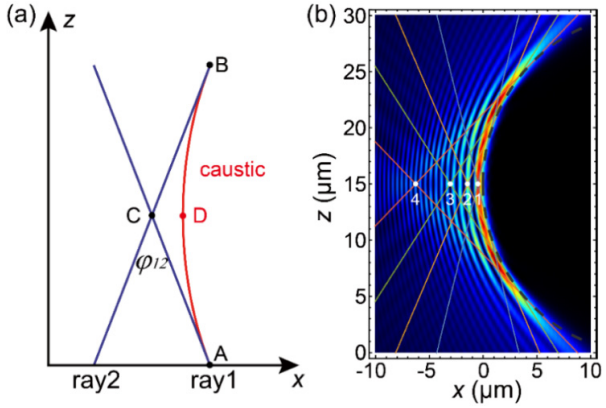

Fig. 3. (a) A two-ray interference model for caustic beams, in which the light field at an arbitrary point C on the left side of the caustic is regarded as the interference of two light rays (ray1 and ray2) tangential to the caustic at point A and point B, respectively. The phase difference of these two light rays at point C is denoted as φ_{12}. (b) The intensity distribution of a circular beam as an instance to demonstrate the relationship between φ_{12} and the local intensity (parameters: $r = x_0 = z_0 = 15\mu m, |k_x| < 0.84k$). The caustic is depicted by a dashed curve and the white dots labeled by 1, 2, 3, 4 correspond to the position of point C in Fig. 3(a) with $\varphi_{12} = 0, 2\pi, 7\pi, 20\pi$.

2.4 Extending caustic beams to nonconvex type

As mentioned in Section 2.2, only the convex type of caustic beams can be constructed based on the above caustic method. In order to extend the caustic beams to the nonconvex type, a

Optics EXPRESS

superposition caustic method has been proposed [26,27]. The idea is to construct several convex (including concave) caustics based on the original caustic method individually, and then superpose them to form an entire nonconvex trajectory, as illustrated in Fig. 4(a). The superposition of all the initial angular spectra for each segment can be generally expressed as

$$A(k_x)=\sum_{j=1}^{n}A_j(k_x)=\sum_{j=1}^{n}r_j(k_x)\exp[i\Phi_j(k_x)], \tag{10}$$

where the index j represents the ordinal of the segments. However, during this superposition, there is actually a degree of freedom in the relative phase between each angular spectrum. Intuitively, the relative phase between the two angular spectra should ensure that the two segments at the joint point has the same phase, namely $\varphi_{FE}=\varphi_F-\varphi_E=0$ as denoted in Fig. 4(a), so that the two segments can joint smoothly, which, however, is actually not the case as shown in Fig. 4(c). It is found that the two segments form a smooth nonconvex main lobe only if $\varphi_{FE}=-\pi/2$ as shown in Figs. 4(b)-4(d), which is also attributed to the additional phase shift $sign[\Psi''(k_{xm})]\cdot\pi/4$ as indicated in Eq. (3). In this case, the interference at the joint point E(F) actually occurs between the light ray tangential to a point right before point E and the light ray tangential to a point right after point F, so there is a $-\pi/2$ phase difference between them similar to Fig. 3(a). In order to ensure these two light rays to interfere in phase at the joint point, a phase shift $\varphi_{FE}=-\pi/2$ should be introduced to the second segment during the superposition in Eq. (10), which is a key in the design of nonconvex caustic beams, otherwise a manual uncertain shift of the relative transverse position of the two segments is required as discussed in [27].

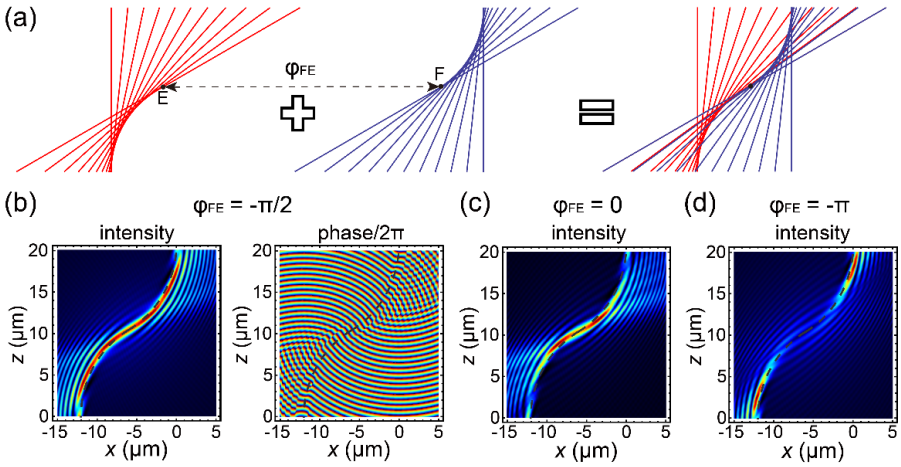

Fig. 4. (a) Schematic showing the concept of superposition caustic method, in which two convex caustics are superposed to form a nonconvex caustic. The phase difference of the two segments at the joint point is denoted as φ_{FE}. A constructed caustic beam by superposing two circular beams, with the phase difference φ_{FE} to be (b) $-\pi/2$, (c) 0, and (d) $-\pi$. The caustic is depicted by a dashed curve (parameters: circle1 : $x=-\sqrt{12^2-z^2}$, circle 2 : $x=\sqrt{12^2-(z-12\sqrt{3})^2}-12, |k_x|<0.98k$, here x and z in units of μm).

3. Restrictions on accelerating beams caustic design

Caustic methods indeed have greatly extended the obtainable propagating trajectories of constructed accelerating beams to most convex and even nonconvex curves, not limited to the

Optics EXPRESS

original parabolic type of Airy beams, so that there is a claim in some previous works that arbitrary trajectories is obtainable based on this design without any restriction. However, this is not the case and we would like to illustrate the restrictions imposed by such caustic methods in the following.

3.1 Constraint in available convex caustic beams

Firstly, we discuss the limitations of constructing accelerating beams propagating along convex trajectories based on the caustic method. As mentioned in Section 2, the light-ray model is based on the stationary phase approximation, which means the above light-ray analysis including the construction of accelerating beams based on caustic methods works only if this approximation is justified. This approximation essentially requires enough spatial frequency ingredients within the integral of Eq. (1), so that the contributions from all these spatial frequencies except the stationary point are canceled out because of fast phase oscillation. However, there isn't such a criterion related to the constructed caustic that can be used to judge whether the caustic will satisfy the approximation and thus obtainable, at present.

Note that the caustic beam can be described by the two-ray interference model as shown in Fig. 3(a). As the point C gradually deviates from the point D on the caustic, the phase difference between the two rays interfering at point C will increase and forms successively the main lobe, the first side lobe, the second side lobe, etc. The maximum phase difference φ_{12} corresponds to the point C where the two rays tangential to the start point and the end point of the caustic, respectively. As this value descends for a caustic, the number of side lobes in the accelerating beam will decrease accordingly and the main lobe will gradually break. A specific instance is presented in Fig. 5, where caustics of an arc with different length corresponding to different φ_{12} as demonstrated are constructed. As the value of φ_{12} descends from 50π, the original well-defined main lobe gradually breaks and finally almost reduces to a symmetric intensity distribution when $\varphi_{12}=0$. Therefore, the constraint for an available curved trajectory of accelerating beams designed by caustic methods can be expressed as

$$\varphi_{12}=k\cdot(l_{\overline{AC}}+l_{\overline{BC}}-l_{\overline{AB}})-\pi/2>>0. \tag{11}$$

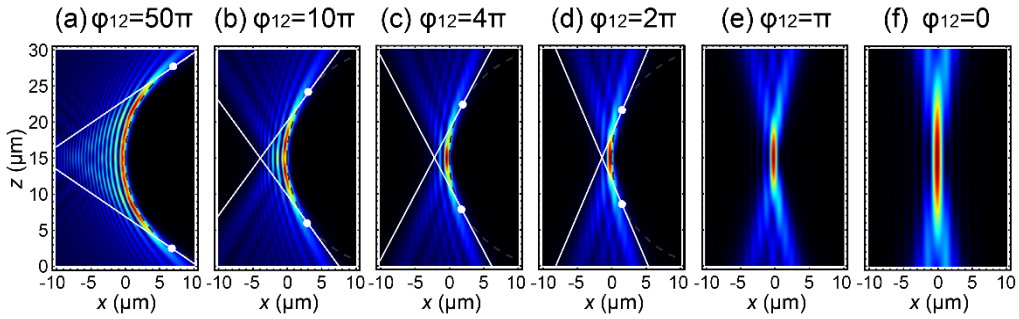

Fig. 5. Intensity distribution of the circular beams as the decrease of φ_{12} corresponding to a decreased length of the designed caustic denoted by the two white dots (parameters: $r=x_0=z_0=15\mu m, |k_x|<0.84k, 0.61k, 0.48k, 0.41k, 0.35k, 0.25k$, respectively). The caustic is depicted by a dashed curve with two rays tangential to its start point and end point.

3.2 Constraint in the available nonconvex caustic beams

As discussed in Section 2.4, accelerating beams propagating along nonconvex trajectories can be constructed based on the superposition caustic method, which superpose several convex caustics designed individually to form an entire nonconvex trajectory. However, after superposition, there will be interference among these convex caustics since the light rays

Optics EXPRESS

forming different segments will intersect as well, as shown in Fig. 6(a), which could break up the entire nonconvex main lobe in certain circumstances.

This problem can be described from the light-ray perspective as illustrated in Fig. 6(a), where two segments of convex caustics are connected to form a nonconvex trajectory. One can see that the ray2 forming the caustic of the second segment unavoidably passes through the caustic of the first segment and therefore will interfere with the ray1 and its neighbouring rays. The interference between these two rays will be constructive and destructive alternatively depending on their phase difference $\Delta\varphi$, which may break the main lobe into several pieces. In order to ensure a smooth main lobe along the nonconvex caustic, the phase difference $\Delta\varphi$ should be kept below π corresponding to the first position of interfering destructively, and therefore the constraint can be expressed as

$$\Delta\varphi = k\cdot(l_{\overset{\frown}{PR}} + l_{\overset{\frown}{RQ}} - l_{\overline{PQ}}) - \pi/2 < \pi, \tag{12}$$

where the additional phase $-\pi/2$ is introduced in the design of nonconvex caustic as discussed in Section 2.4. To justify the above formula, we superpose two circular caustics to form the nonconvex caustic beams as shown in Figs. 6(b) and 6(c). As the radius of the circular caustic increases, it is noted that the intensity of the main lobe is no longer smooth along the whole nonconvex trajectory, and the breakup position almost matches the point with a phase difference $\Delta\varphi = \pi$ as denoted by the end points of the depicted caustic, which confirms the above constraint for an available smooth nonconvex trajectory of accelerating beams designed by superposition caustic methods.

Apart from the 2D cases discussed in this work, accelerating beams in 3D space are also available by associating the propagating trajectories with 3D caustics, which have been demonstrated recently [24,29]. In the 3D case, the problem of interference or intersection between light rays tangential to a caustic discussed above can be easily avoided and thus a smooth main lobe can be obtained without breaking up into pieces, while there also exists another inherent constraint as discussed in [24].

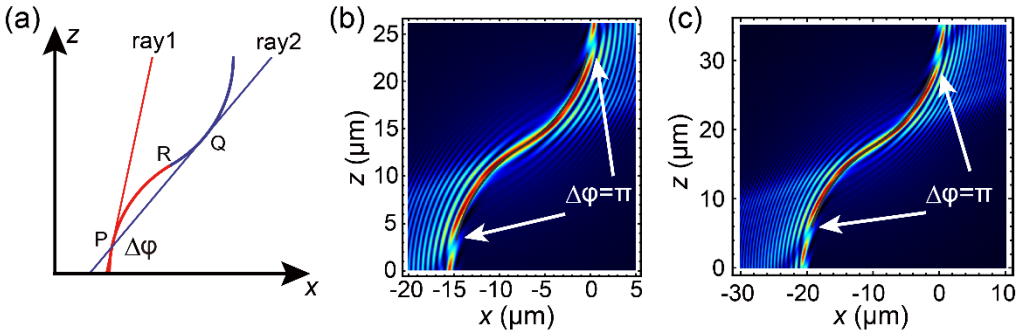

Fig. 6. (a) Schematic showing two-ray interference in the construction of a nonconvex caustic with a joint point R. Ray2 tangential to the second segment in blue (at tangential point Q) will pass through the first segment at point P and thus interfere with ray1, the phase difference of these two rays are denoted as $\Delta\varphi$. Intensity distributions of constructed nonconvex beams composed of two circular caustics in radius of (b) 15 μm (parameters: $\text{circle}\,1: x = -\sqrt{15^2 - z^2}$, $\text{circle}\,2: x = \sqrt{15^2 - (z - 15\sqrt{3})^2} - 15, |k_x| < 0.98k$, here x and z in units of μm) and (c) 20 μm (parameters: $\text{circle}\,1: x = -\sqrt{20^2 - z^2}$, $\text{circle}\,2: x = \sqrt{20^2 - (z - 20\sqrt{3})^2} - 20, |k_x| < 0.98k$, here x and z in units of μm), respectively. The nonconvex caustics are shown in grey curves, with the start and end point corresponding to $\Delta\varphi = \pi$.

Optics EXPRESS

4. Conclusion

In summary, we firstly elaborate the Fourier-space light ray model and caustic method for the design of 2D accelerating beams propagating along both convex and nonconvex trajectories, respectively. It is found that caustic design enables the constructed light beam to possess not simply a curved intensity distribution as well-known, but also a linear phase distribution along the caustic, equivalent to the phase accumulation due to moving along a curved path, which is an interesting and useful characteristic for the light-ray analysis. From this light-ray perspective, we further analyze the restrictions of the above caustic design in constructing different types of accelerating beams and illustrate constraints in each case, including 2D convex and nonconvex caustic beams. We anticipate that the full analysis of the caustic method for the design of accelerating beams including its construction, characteristics, and constraints may clarify, inspire, and thus advance the development of such method, which will certainly benefit a variety of applications based on accelerating beams.

Funding

National Natural Science Foundation of China (NSFC) (11774437, U1701661, 61490715); Science and Technology Program of Guangzhou (201804010302); Local Innovative and Research Teams Project of Guangdong Pearl River Talents Program (2017BT01X121); Fundamental Research Funds for the Central Universities of China (SYSU: 17lgzd06).

Appendix A: Derivation of the phase distribution along the caustic

Based on Eqs. (2) and (5), we have

$$\Phi'(k_{x1}) = \frac{k_{x1}}{(k^2 - k_{x1}^2)^{1/2}} z - x = zf'(z) - f(z). \tag{13}$$

After integrating with k_{x1}, the phase of the angular spectrum mapping to each point on the caustic can be expressed as

$$\begin{aligned}\Phi(k_{x1}) &= \int zf'(z) - f(z)dk_{x1} = k_{x1}[zf'(z) - f(z)] - \int k_{x1} d[zf'(z) - f(z)] \\ &= \frac{kf'(z)[zf'(z) - f(z)]}{\sqrt{1+[f'(z)]^2}} - \int \frac{kf'(z)\cdot zf''(z)}{\sqrt{1+[f'(z)]^2}} dz.\end{aligned} \tag{14}$$

Therefore, the phase on the caustic is

$$\begin{aligned}\Psi(k_{x1}) &= k_{x1}x + (k^2 - k_{x1}^2)^{1/2} z + \Phi(k_{x1}) \\ &= \frac{kf'(z)\cdot f(z)}{\sqrt{1+[f'(z)]^2}} + \frac{k\cdot z}{\sqrt{1+[f'(z)]^2}} + \frac{kf'(z)[zf'(z) - f(z)]}{\sqrt{1+[f'(z)]^2}} - \int \frac{kf'(z)\cdot zf''(z)}{\sqrt{1+[f'(z)]^2}} dz \\ &= kz\sqrt{1+[f'(z)]^2} - \int \frac{kf'(z)\cdot zf''(z)}{\sqrt{1+[f'(z)]^2}} dz \\ &= kz\sqrt{1+[f'(z)]^2} - k\int z d\left\{\sqrt{1+[f'(z)]^2}\right\} \\ &= k\int \sqrt{1+[f'(z)]^2} dz.\end{aligned} \tag{15}$$

References

1. H. Rubinsztein-Dunlop, A. Forbes, M. V. Berry, M. R. Dennis, D. L. Andrews, M. Mansuripur, C. Denz, C. Alpmann, P. Banzer, T. Bauer, E. Karimi, L. Marrucci, M. Padgett, M. Ritsch-Marte, N. M. Litchinitser, N. P. Bigelow, C. Rosales-Guzmán, A. Belmonte, J. P. Torres, T. W. Neely, M. Baker, R. Gordon, A. B. Stilgoe, J.

Optics EXPRESS

Romero, A. G. White, R. Fickler, A. E. Willner, G. Xie, B. McMorran, and A. M. Weiner, "Roadmap on structured light," J. Opt. **19**(1), 013001 (2017).
2. G. A. Siviloglou and D. N. Christodoulides, "Accelerating finite energy Airy beams," Opt. Lett. **32**(8), 979–981 (2007).
3. G. A. Siviloglou, J. Broky, A. Dogariu, and D. N. Christodoulides, "Observation of accelerating Airy beams," Phys. Rev. Lett. **99**(21), 213901 (2007).
4. J. Durnin, J. Miceli, Jr., and J. H. Eberly, "Diffraction-free beams," Phys. Rev. Lett. **58**(15), 1499–1501 (1987).
5. L. Allen, M. W. Beijersbergen, R. J. C. Spreeuw, and J. P. Woerdman, "Orbital angular momentum of light and the transformation of Laguerre-Gaussian laser modes," Phys. Rev. A **45**(11), 8185–8189 (1992).
6. H. E. Kondakci and A. F. Abouraddy, "Airy wave packets accelerating in space-time," Phys. Rev. Lett. **120**(16), 163901 (2018).
7. Z. Chen, J. Xu, Y. Hu, and D. Song, "Control and novel applications of self-accelerating beams," Acta Opt. Sin. **36**(10), 1026009 (2016).
8. W. Wen and Y. Cai, "Research progress of generation characteristics and applications of self-accelerating Airy beams," Laser & Optoelectronics Progress **54**(2), 020002 (2017).
9. I. Kaminer, R. Bekenstein, J. Nemirovsky, and M. Segev, "Nondiffracting accelerating wave packets of Maxwell's equations," Phys. Rev. Lett. **108**(16), 163901 (2012).
10. P. Zhang, Y. Hu, T. Li, D. Cannan, X. Yin, R. Morandotti, Z. Chen, and X. Zhang, "Nonparaxial Mathieu and Weber accelerating beams," Phys. Rev. Lett. **109**(19), 193901 (2012).
11. A. Mathis, F. Courvoisier, L. Froehly, L. Furfaro, M. Jacquot, P. A. Lacourt, and J. M. Dudley, "Micromachining along a curve: femtosecond laser micromachining of curved profiles in diamond and silicon using accelerating beams," Appl. Phys. Lett. **101**(7), 071110 (2012).
12. J. Baumgartl, M. Mazilu, and K. Dholakia, "Optically mediated particle clearing using Airy wavepackets," Nat. Photonics **2**(11), 675–678 (2008).
13. J. Zhao, I. D. Chremmos, D. Song, D. N. Christodoulides, N. K. Efremidis, and Z. Chen, "Curved singular beams for three-dimensional particle manipulation," Sci. Rep. **5**(1), 12086 (2015).
14. Y. Liang, Y. Hu, D. Song, C. Lou, X. Zhang, Z. Chen, and J. Xu, "Image signal transmission with Airy beams," Opt. Lett. **40**(23), 5686–5689 (2015).
15. G. Zhu, Y. Wen, X. Wu, Y. Chen, J. Liu, and S. Yu, "Obstacle evasion in free-space optical communications utilizing Airy beams," Opt. Lett. **43**(6), 1203–1206 (2018).
16. S. Jia, J. C. Vaughan, and X. Zhuang, "Light-sheet microscopy using an Airy beam," Nat. Photonics **8**, 302–306 (2014).
17. T. Vettenburg, H. I. C. Dalgarno, J. Nylk, C. Coll-Lladó, D. E. K. Ferrier, T. Čižmár, F. J. Gunn-Moore, and K. Dholakia, "Light-sheet microscopy using an Airy beam," Nat. Methods **11**(5), 541–544 (2014).
18. P. Polynkin, M. Kolesik, J. V. Moloney, G. A. Siviloglou, and D. N. Christodoulides, "Curved plasma channel generation using ultraintense Airy beams," Science **324**(5924), 229–232 (2009).
19. M. Clerici, Y. Hu, P. Lassonde, C. Milián, A. Couairon, D. N. Christodoulides, Z. Chen, L. Razzari, F. Vidal, F. Légaré, D. Faccio, and R. Morandotti, "Laser-assisted guiding of electric discharges around objects," Sci. Adv. **1**(5), e1400111 (2015).
20. Y. Wen, Y. Chen, and S. Yu, "Design of accelerating beams based on caustic method," Acta Phys. Sin. **66**, 144210 (2017).
21. M. Berry and C. Upstill, *Catastrophe Optics: Morphologies of Caustic and Their Diffraction Patterns* (Elsevier, 1980).
22. E. Greenfield, M. Segev, W. Walasik, and O. Raz, "Accelerating light beams along arbitrary convex trajectories," Phys. Rev. Lett. **106**(21), 213902 (2011).
23. Y. Hu, D. Bongiovanni, Z. Chen, and R. Morandotti, "Multipath multicomponent self-accelerating beams through spectrum-engineered position mapping," Phys. Rev. A **88**(4), 043809 (2013).
24. Y. Wen, Y. Chen, Y. Zhang, H. Chen, and S. Yu, "Tailoring accelerating beams in phase space," Phys. Rev. A **95**(2), 023825 (2017).
25. L. Froehly, F. Courvoisier, A. Mathis, M. Jacquot, L. Furfaro, R. Giust, P. A. Lacourt, and J. M. Dudley, "Arbitrary accelerating micron-scale caustic beams in two and three dimensions," Opt. Express **19**(17), 16455–16465 (2011).
26. Y. Wen, Y. Chen, Y. Zhang, H. Chen, and S. Yu, "Winding light beams along elliptical helical trajectories," Phys. Rev. A **94**(1), 013829 (2016).
27. T. Melamed and A. Shlivinski, "Practical algorithm for custom-made caustic beams," Opt. Lett. **42**(13), 2499–2502 (2017).
28. M. A. Bandres, M. A. Alonso, I. Kaminer, and M. Segev, "Three-dimensional accelerating electromagnetic waves," Opt. Express **21**(12), 13917–13929 (2013).
29. Y. Wen, Y. Chen, Y. Zhang, and S. Yu, "Highly adjustable helical beam: design and propagation characteristics," Chin. Opt. Lett. **15**(3), 030011 (2017).
30. R. Schley, I. Kaminer, E. Greenfield, R. Bekenstein, Y. Lumer, and M. Segev, "Loss-proof self-accelerating beams and their use in non-paraxial manipulation of particles' trajectories," Nat. Commun. **5**(1), 5189 (2014).
31. M. Gooutsoulas and N. K. Efremidis, "Precise amplitude, trajectory, and beam-width control of accelerating and abruptly autofocusing beams," Phys. Rev. A **97**(6), 063831 (2018).
32. R. Wong, *Asymptotic approximations of integrals* (Academic, 1989).

Optics EXPRESS

33. P. Vaveliuk, A. Lencina, J. A. Rodrigo, and O. M. Matos, "Caustics, catastrophes, and symmetries in curved beams," Phys. Rev. A **92**(3), 033850 (2015).
34. J. F. Nye, *Natural Focusing and Fine Structure of Light: Caustics and Wave Dislocations* (Institute of Physics Publishing, 1999).